Solar CO_2 Reduction

Deutsche Ausgabe: DOI: 10.1002/ange.201506966
Internationale Ausgabe: DOI: 10.1002/anie.201506966

Single Unit Cell Bismuth Tungstate Layers Realizing Robust Solar CO_2 Reduction to Methanol

Liang Liang, Fengcai Lei, Shan Gao, Yongfu Sun, Xingchen Jiao, Ju Wu, Shaista Qamar, and Yi Xie**

Abstract: *Solar CO_2 reduction into hydrocarbons helps to solve the global warming and energy crisis. However, conventional semiconductors usually suffer from low photoactivity and poor photostability. Here, atomically-thin oxide-based semiconductors are proposed as excellent platforms to overcome this drawback. As a prototype, single-unit-cell Bi_2WO_6 layers are first synthesized by virtue of a lamellar Bi-oleate intermediate. The single-unit-cell thickness allows 3-times larger CO_2 adsorption capacity and higher photoabsorption than bulk Bi_2WO_6. Also, the increased conductivity, verified by density functional theory calculations and temperature-dependent resistivities, favors fast carrier transport. The carrier lifetime increased from 14.7 to 83.2 ns, revealed by time-resolved fluorescence spectroscopy, which accounts for the improved electron-hole separation efficacy. As a result, the single-unit-cell Bi_2WO_6 layers achieve a methanol formation rate of 75 $\mu mol\, g^{-1} h^{-1}$, 125-times higher than that of bulk Bi_2WO_6. The catalytic activity of the single-unit-cell layers proceeds without deactivation even after 2 days. This work will shed light on designing efficient and robust photoreduction CO_2 catalysts.*

Fossil fuels currently comprise over 80% of global energy sources, and their continued use unfortunately contributes to the rising levels of atmospheric carbon dioxide. To realize the sustainable development of society, the overly produced CO_2 should be converted into reusable carbon forms. In this respect, artificial photosynthesis, which directly converts CO_2 and water on photocatalysts into valuable fuels using sunlight at room temperature and ambient pressure, has been regarded as one of the most promising and compelling strategies for simultaneously solving the energy and environmental problems.[1] Although a few photocatalysts, such as sulfides, phosphides, and nitrides have been reported to be active for CO_2 photoconversion,[2] these materials usually undergo serious photocorrosion under solar illumination in an aqueous environment. In contrast, oxide-based semiconductors are often more thermodynamically stable, and hence would be suitable candidates for solar-driven CO_2 conversion. Among these catalytic materials, orthorhombic Bi_2WO_6 has emerged as a promising candidate. Orthorhombic Bi_2WO_6 is naturally abundant and non-toxic. Furthermore, the fascination of orthorhombic Bi_2WO_6 also comes from its peculiar structure, constructed by alternating fluorine-like layers $(Bi_2O_2)^{2+}$ and perovskite layers $(WO_4)^{2-}$,[3] which endows it with high chemical and thermal stability. Importantly, the orthorhombic Bi_2WO_6 has a suitable conduction band potential capable of CO_2 reduction, which makes it to be a favorable photocatalyst for reduction of CO_2 into renewable hydrocarbon fuel.[3,4] In spite of these advantages, orthorhombic Bi_2WO_6 usually suffers from low CO_2 photoconversion efficiency,[3,4] which is primarily ascribed to its inherently poor electrical conductivity and very low exposed surface active sites. Therefore, fabricating oxide-based semiconductors with abundant active sites and increased conductivity is highly desirable and imperative for efforts to achieve highly efficient solar CO_2 conversion into fuels.

Herein, atomically-thin oxide-based semiconductors are proposed as an excellent platform to promote solar CO_2 conversion by affording abundant catalytically active sites, increased two-dimensional conductivity, and superior structural stability. Taking the orthorhombic Bi_2WO_6 as a prototype, the atomic-scale thickness could provide an extremely large fraction of low-coordinated surface atoms,[5] which could act as the catalytic sites to trigger CO_2 reduction reactions. Also, the ultra-large specific surface area allows for efficiently harnessing solar energy,[6] while the ultrathin thickness enables the photo-excited carriers to be easily transferred from the interior to the surface, and hence decreases the bulk recombination according to the diffusion formula of $t = d^2/k^2D$ (d is the particle size, k is a constant, D is the diffusion coefficient of electron-hole pairs).[7] More importantly, once the thickness of orthorhombic Bi_2WO_6 is down to single-unit cell, density-functional-theory (DFT) calculations reveal that it possesses an increased density of states (DOS) at the conduction band edge as compared with its bulk counterpart (Figure 1 A,B),[8] which is further demonstrated by the corresponding distribution of charge density. More importantly, as revealed by the spatial distribution of charge density near the Fermi level (Figure 1 C,D; Supporting Information, Figure S1), the vast majority of charge density concentrates on the surface of the single-unit-cell Bi_2WO_6 layer slab, which means that the active electrons mainly come from the surface atomic layer upon reducing the dimensionality from 3D bulk Bi_2WO_6 to the atomically-thin Bi_2WO_6 layers. Thus, the photoexcited electron-hole pairs would take

[*] L. Liang,[+] F. Lei,[+] S. Gao, Prof. Y. Sun, X. Jiao, J. Wu, S. Qamar, Prof. Y. Xie
Hefei National Laboratory for Physical Sciences at Microscale
Collaborative Innovation Center of Chemistry for Energy Materials
University of Science & Technology of China
Hefei, Anhui 230026 (P.R. China)
E-mail: yfsun@ustc.edu.cn
yxie@ustc.edu.cn

[+] These authors contributed equally to this work.

Supporting information for this article is available on the WWW under http://dx.doi.org/10.1002/anie.201506966.

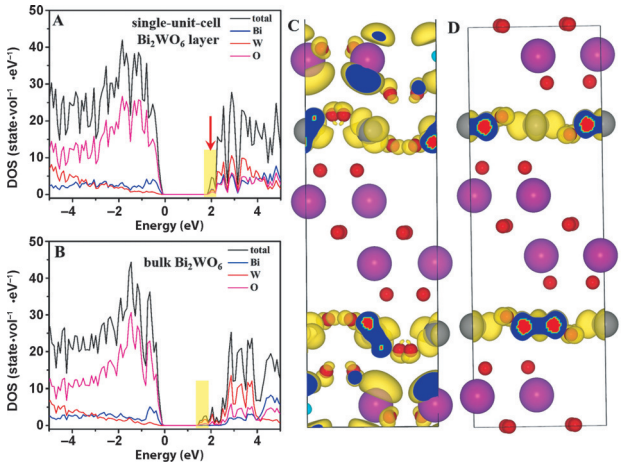

Figure 1. DFT calculations. Calculated density of states of (A) single-unit-cell Bi_2WO_6 layer slab and (B) bulk Bi_2WO_6 slab. Charge density distribution for the conduction band edge of (C) single-unit-cell Bi_2WO_6 layer slab and (D) bulk Bi_2WO_6 slab.

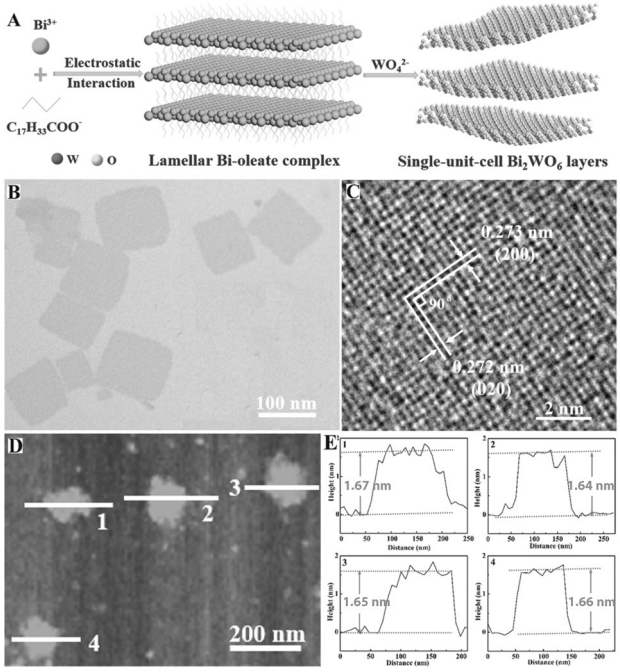

Figure 2. (A) Illustration of the formation of single-unit-cell Bi_2WO_6 layers. Characterizations for the single-unit-cell Bi_2WO_6 layers: (B) TEM image, (C) HRTEM image, (D) AFM image, and (E) the corresponding height profiles; the numbers from 1 to 4 in (D) correspond to the numbers from 1 to 4 in (E).

less time to reach the surface than those generated deeply in the bulk Bi_2WO_6, which helps to reduce their recombination rates and thereby effectively promotes solar CO_2 reduction. Inspired by the aforementioned concepts, the controllable synthesis of orthorhombic single-unit cell Bi_2WO_6 layers is of vital importance and practical significance. However, for the orthorhombic Bi_2WO_6 with little anisotropy, the difficulty in bond-cleavage and the lack of intrinsic driving forces for 2D anisotropic growth lead the fabrication of its atomic-layers to be a challenge. Therefore, it is highly desirable to develop a convenient pathway to synthesize ultrathin orthorhombic Bi_2WO_6 atomic layers.

Herein, we proposed a lamellar hybrid intermediate strategy for successfully synthesizing single-unit-cell Bi_2WO_6 layers, taking advantage of an intermediate precursor of lamellar Bi-oleate complex. Note that oleate ions played an important role in the formation of this lamellar intermediate, in which the oleate ions initially interacted with Bi^{3+} to form lamellar Bi-oleate complexes through the self-assembly process (Figure 2A),[8a,9] confirmed by the corresponding small-angle XRD pattern (Supporting Information, Figure S2). After the addition of Na_2WO_4 followed by hydrothermal treatment, single-unit-cell Bi_2WO_6 layers were yielded, which were fully characterized as follows. The XRD pattern (Supporting Information, Figure S3A) for the accumulated powder sample could be readily indexed to orthorhombic Bi_2WO_6 (JCPDS No. 73-2020). Meanwhile, the XPS spectra (Supporting Information, Figure S3B–D) demonstrated the formation of pure Bi_2WO_6,[3] which was further shown by the corresponding IR spectrum (Supporting Information, Figure S4),[10] implying the absence of oleate ions on the surface of the as-synthesized products. TEM images (Figure 2B) clearly depicted their sheet-like morphology with average lateral size of 100 nm, while the HRTEM image (Figure 2C) revealed their orientation along the [001] projection. Atomic force microscopic (AFM) imaging and the corresponding height profiles showed an average thickness of 1.65 nm (Figure 2D,E), which was in agreement with the 1.64 nm thickness of a unit cell along the [001] direction. Thus, the above results demonstrated the formation of clean Bi_2WO_6 atomic layers with a unit cell thickness.

The Bi_2WO_6 atomic layers would exhibit unprecedented CO_2 photocatalytic properties owing to the single unit cell thickness, higher specific surface area (27.6 vs. 0.7 m^2g^{-1}), increased DOS near the Fermi level, and enhanced charge density on the surface. The CO_2 photoreduction experiments were carried out in water under a 300-W Xe lamp with a standard AM 1.5G filter, and the predominant reaction product analyzed by gas chromatography (GC) was methanol. The methanol yield gradually increased with the photolysis time, and the total yield of methanol obtained in the experiment after 5 h of continuous irradiation was 451.7 $\mu mol\,g^{-1}$, corresponding to approximately 75 $\mu mol\,g^{-1}h^{-1}$ of the methanol formation rate, which was 3- and 125-times higher than that of the Bi_2WO_6 nanocrystals (23 $\mu mol\,g^{-1}h^{-1}$) and bulk Bi_2WO_6 (0.6 $\mu mol\,g^{-1}h^{-1}$), respectively (Supporting Information, Figures S5, S6). Such a high methanol formation rate is also much larger than that of previously reported TiO_2 loaded zeolite (5.5 $\mu mol\,g^{-1}h^{-1}$),[11] and Ag/TiO_2 (4.12 $\mu mol\,g^{-1}h^{-1}$),[12] which strongly demonstrated the superior photocatalytic activity of the ultrathin oxide-semiconductor atomic layers. Furthermore, control experiments demonstrated that there was no detectable methanol generation in the dark or in the absence of photocatalysts, further verifying that the CO_2 reduction reaction is indeed driven under artificial irradiation with a photocatalyst. More importantly, the CO_2 photo-reduction activity of the recycled single-unit-cell Bi_2WO_6 layers sample

did not exhibit any significant loss of photocatalytic activity after the sixth cycle of repetition tests for photocatalytic reduction of CO_2 (Figure 3B), which strongly confirmed their excellent photostability (Supporting Information, Figure S7), giving prospective signs for practical solar fuels production.

The significantly improved CO_2 photo-reduction properties of the single-unit-cell Bi_2WO_6 layers could be primarily ascribed to their unique geometric structure (Figure 4). When the thickness is down to a single-unit-cell, the ultra-large surface area for the single-unit-cell Bi_2WO_6 layers favors the enhancement of CO_2 adsorption capacity (Figure 4A), thus providing the prerequisite to participate in the following

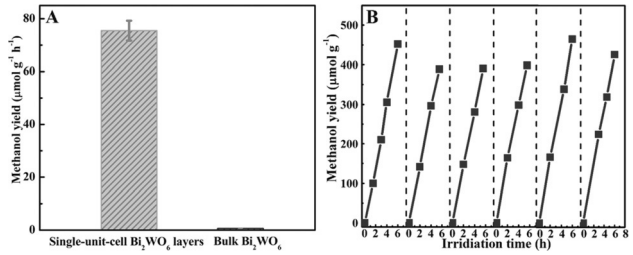

Figure 3. Photocatalytic methanol evolution under 300 W Xe lamp irradiation for single-unit-cell Bi_2WO_6 layers and bulk Bi_2WO_6. (A) Methanol formation rate, (B) cycling curves. The error bars in A represent the standard deviations of three independent measurements of the same sample.

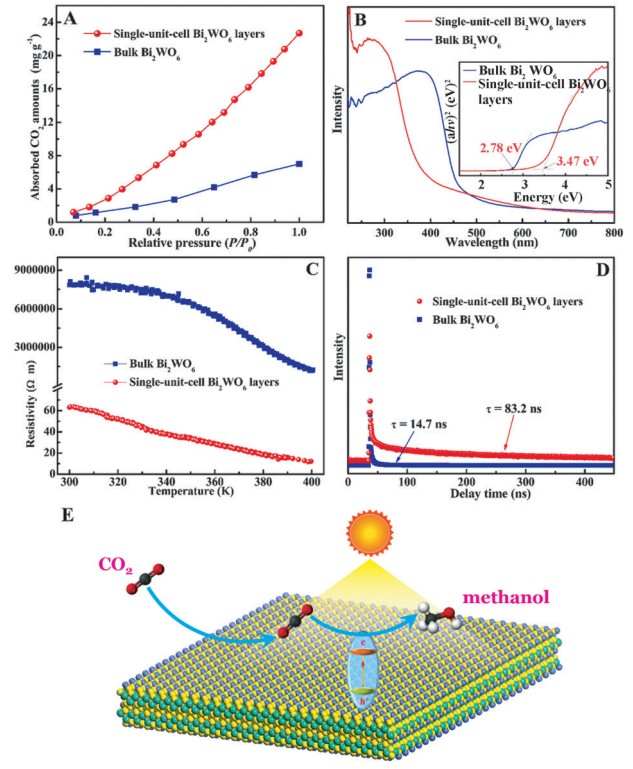

Figure 4. (A) CO_2 adsorption isotherms, (B) UV/Vis diffuse reflectance spectra, (C) temperature-dependent resistivities and (D) fluorescence emission decay spectra for the single-unit-cell Bi_2WO_6 layers and bulk Bi_2WO_6. (E) Illustration of the solar-driven CO_2 reduction into methanol on the single-unit-cell Bi_2WO_6 layers.

reactions. For example, the CO_2 adsorption isotherms clearly depict that the amount of CO_2 adsorption capacity at 298 K and 1 atm over single-unit-cell Bi_2WO_6 layers could reach 22.7 mg g^{-1}, which is over 3-times higher than that of the bulk counterpart (7 mg g^{-1}). Furthermore, the ultrathin Bi_2WO_6 layers possess increased photoabsorption in the UV region compared with the bulk counterpart (Figure 4B), which could be attributed to their extremely large surface area that allows absorption to happen quickly and efficiently.[5a,6a,8a] Moreover, the temperature-dependent resistivity indicates that the single-unit-cell Bi_2WO_6 layers exhibit dramatically higher electronic conductivity relative to the bulk counterpart (Figure 4C), which is consistent with their increased DOS near the Fermi level (Figure 1). The enhanced electronic conductivity would benefit the transport of photogenerated carriers, which retard the recombination rate of the carriers. The single-unit-cell thickness also enables the rapid transfer of charge carriers from the interior onto the surface, which facilitates the separation of photogenerated electron and hole, and thereby further decreases the bulk recombination rate and simultaneously increases the lifetime of the carriers.[13] This could be further demonstrated by time-resolved fluorescence emission decay spectra (Figure 4D). The decay kinetics for single-unit-cell Bi_2WO_6 layers is much slower than that of bulk counterpart, in which their respective average fluorescence lifetimes are 83.2 and 14.7 ns, suggesting that the former could effectively reduce the recombination of the charge carriers.[14]

In conclusion, atomic layers for oxide-based semiconductors are put forward as an excellent platform to promote solar CO_2 conversion by affording abundant catalytic sites, increased two-dimensional conductivity, and superior structural stability. As an example, single-unit-cell Bi_2WO_6 layers are first synthesized by virtue of a lamellar Bi-oleate intermediate. CO_2 adsorption isotherms and UV/Vis diffuse reflectance spectra reveal that the ultra-large surface area endows Bi_2WO_6 atomic-layers with 3-times higher CO_2 adsorption capacity and larger photoabsorption relative to bulk Bi_2WO_6. Time-resolved fluorescence emission spectra disclose that the single-unit-cell thickness helps to increase the carriers lifetime from 14.7 to 83.2 ns. DFT calculations demonstrate the increased DOS at the conduction band edge, while the vast majority of charge density concentrates on the surface, which benefits the two-dimensional conductivity as verified by their temperature-dependent resistivities. As a result, the single-unit-cell Bi_2WO_6 layers achieve a methanol formation rate of 75 μmol g^{-1} h^{-1}, 125-times higher than that of the bulk Bi_2WO_6 and also over 10-times higher than that of previously reported TiO_2-loaded zeolite and Ag/TiO_2. More importantly, the catalytic activity for single-unit-cell Bi_2WO_6 layers does not show any obvious deactivation even after 2 days of photocatalysis. In brief, this study may open new opportunities for designing highly efficient and robust solar-driven CO_2 conversion catalysts.

Acknowledgements

This work was financially supported by National Nature Science Foundation (21331005, 21422107, 21201157, 91422303, 11321503), Program for New Century Excellent Talents in University (NCET-13-0546), Youth Innovation Promotion Association of CAS (CX2340000100) and the Fundamental Research Funds for the Central Universities No. WK2340000063.

Keywords: atomic-layers · bismuth tungstate · methanol · solar CO_2 reduction

How to cite: *Angew. Chem. Int. Ed.* **2015**, *54*, 13971–13974
Angew. Chem. **2015**, *127*, 14177–14180

[1] a) S. C. Roy, O. K. Varghese, M. Paulose, C. A. Grimes, *ACS Nano* **2010**, *4*, 1259; b) T. Sakakura, J. C. Choi, H. Yasuda, *Chem. Rev.* **2007**, *107*, 2365–2387; c) K. Iizuka, T. Wato, Y. Miseki, K. Saito, A. Kudo, *J. Am. Chem. Soc.* **2011**, *133*, 20863.

[2] a) K. F. Li, X. Q. An, K. H. Park, M. Khraisheh, J. W. Tang, *Catal. Today* **2014**, *224*, 3; b) S. Sato, T. Arai, T. Morikawa, K. Uemura, T. M. Suzuki, H. Tanaka, T. Kajino, *J. Am. Chem. Soc.* **2011**, *133*, 15240; c) M. Halmann, *Nature* **1978**, *275*, 115.

[3] Y. Zhou, Z. P. Tian, Z. Y. Zhao, Q. Liu, J. H. Kou, X. Y. Chen, J. Gao, S. C. Yan, Z. G. Zou, *ACS Appl. Mater. Interfaces* **2011**, *3*, 3594.

[4] H. F. Cheng, B. B. Huang, Y. Y. Liu, Z. Y. Wang, X. Y. Qin, X. Y. Zhang, Y. Dai, *Chem. Commun.* **2012**, *48*, 9729.

[5] a) Y. F. Sun, Z. H. Sun, S. Gao, H. Cheng, Q. H. Liu, J. Y. Piao, T. Yao, C. Z. Wu, S. L. Hu, S. Q. Wei, Y. Xie, *Nat. Commun.* **2012**, *3*, 1057; b) Y. F. Sun, Q. H. Liu, S. Gao, H. Cheng, F. C. Lei, Z. H. Sun, Y. Jiang, H. B. Su, S. Q. Wei, Y. Xie, *Nat. Commun.* **2013**, *4*, 2899; c) Y. F. Sun, F. C. Lei, S. Gao, B. C. Pan, J. F. Zhou, Y. Xie, *Angew. Chem. Int. Ed.* **2013**, *52*, 10569; *Angew. Chem.* **2013**, *125*, 10763.

[6] a) Y. F. Sun, H. Cheng, S. Gao, Z. H. Sun, Q. H. Liu, Q. Liu, F. C. Lei, T. Yao, J. F. He, S. Q. Wei, Y. Xie, *Angew. Chem. Int. Ed.* **2012**, *51*, 8727–8731; *Angew. Chem.* **2012**, *124*, 8857; b) Y. F. Sun, Z. H. Sun, S. Gao, H. Cheng, Q. H. Liu, F. C. Lei, S. Q. Wei, Y. Xie, *Adv. Energy Mater.* **2014**, *4*, 1300611.

[7] R. L. Bickley, G. C. Williams, *Mater. Chem. Phys.* **1997**, *51*, 47.

[8] a) F. C. Lei, Y. F. Sun, K. T. Liu, S. Gao, L. Liang, B. C. Pan, Y. Xie, *J. Am. Chem. Soc.* **2014**, *136*, 6826; b) Y. F. Sun, H. Cheng, S. Gao, Q. H. Liu, Z. H. Sun, C. Xiao, C. Z. Wu, S. P. Wei, Y. Xie, *J. Am. Chem. Soc.* **2012**, *134*, 20294.

[9] a) S. Gao, Y. F. Sun, F. C. Lei, J. W. Liu, L. Liang, T. W. Li, B. C. Pan, J. F. Zhou, Y. Xie, *Nano Energy* **2014**, *8*, 205; b) Y. F. Sun, Y. Xie, C. Z. Wu, S. D. Zhang, S. S. Jiang, *Nano Res.* **2010**, *3*, 620.

[10] M. Maczka, J. Hanuza, W. Paraguassu, A. G. S. Filho, P. T. C. Freire, J. M. Filho, *Appl. Phys. Lett.* **2008**, *92*, 112911.

[11] M. Anpo, H. Yamashita, Y. Ichihashi, Y. Fujii, M. Honda, *J. Phys. Chem. B* **1997**, *101*, 2632.

[12] J. C. S. Wu, T.-H. Wu, T. Chu, H. Huang, D. Tsai, *Top. Catal.* **2008**, *47*, 131.

[13] F. C. Lei, L. Zhang, Y. F. Sun, L. Liang, K. T. Liu, J. Q. Xu, Q. Zhang, B. C. Pan, Y. Luo, Y. Xie, *Angew. Chem. Int. Ed.* **2015**, *54*, 9266; *Angew. Chem.* **2015**, *127*, 9398.

[14] S. M. Sun, W. Z. Wang, D. Jiang, L. Zhang, X. M. Li, Y. L. Zheng, Q. An, *Nano Res.* **2014**, *7*, 1497.

Received: July 27, 2015
Published online: September 30, 2015